

## Research



**Cite this article:** MacLaren JA, Bennion RF, Bardet N, Fischer V. 2022 Global ecomorphological restructuring of dominant marine reptiles prior to the Cretaceous–Palaeogene mass extinction. *Proc. R. Soc. B* **289**: 20220585.  
<https://doi.org/10.1098/rspb.2022.0585>

Received: 26 March 2022

Accepted: 3 May 2022

**Subject Category:**

Palaeobiology

**Subject Areas:**

evolution, palaeontology, ecology

**Keywords:**

Mosasauroidea, morphometrics, provincialism, megapredator, ecomorphology, Cretaceous

**Author for correspondence:**

Jamie A. MacLaren

e-mail: [j.maclaren@uliege.be](mailto:j.maclaren@uliege.be)

Electronic supplementary material is available online at <https://doi.org/10.6084/m9.figshare.c.5986026>.

# Global ecomorphological restructuring of dominant marine reptiles prior to the Cretaceous–Palaeogene mass extinction

Jamie A. MacLaren<sup>1,2</sup>, Rebecca F. Bennion<sup>1,3</sup>, Nathalie Bardet<sup>4</sup> and Valentin Fischer<sup>1</sup>

<sup>1</sup>Evolution and Diversity Dynamics Lab, UR Geology, Université de Liège, 14 Allée du 6 Août, Liège 4000, Belgium

<sup>2</sup>Functional Morphology Lab, Department of Biology, Universiteit Antwerpen, Gebouw D, Campus Drie Eiken, Universiteitsplein 1, Wilrijk, Antwerpen 2610, Belgium

<sup>3</sup>O.D. Terre et Histoire de la Vie, Institut Royal des Sciences Naturelles de Belgique, Rue Vautier 29, Brussels 1000, Belgium

<sup>4</sup>CR2P – Centre de Recherche en Paléontologie de Paris, UMR 7207 CNRS-MNHN-SU, Muséum National d'Histoire Naturelle, 57 Rue Cuvier, CP38, Paris 75005, France

**id** JAM, 0000-0003-4177-227X; RFB, 0000-0002-0910-1655; VF, 0000-0002-8808-6747

Mosasaurid squamates were the dominant amniote predators in marine ecosystems during most of the Late Cretaceous. Here, we use a suite of biomechanically rooted, functionally descriptive ratios in a framework adapted from population ecology to investigate how the morphofunctional disparity of mosasaurids evolved prior to the Cretaceous–Palaeogene (K/Pg) mass extinction. Our results suggest that taxonomic turnover in mosasaurid community composition from Campanian to Maastrichtian is reflected by a notable global increase in morphofunctional disparity, especially driving the North American record. Ecomorphospace occupation becomes polarized during the late Maastrichtian, with morphofunctional disparity plateauing in the Southern Hemisphere and decreasing in the Northern Hemisphere. We show that these changes are not strongly associated with mosasaurid size, but rather with the functional capacities of their skulls. Our novel approach indicates that mosasaurid morphofunctional disparity was in decline in multiple provincial communities before the K/Pg mass extinction, highlighting region-specific patterns of disparity evolution and the importance of assessing vertebrate extinctions both globally and locally. Ecomorphological differentiation in mosasaurid communities, coupled with declines in other formerly abundant marine reptile groups, indicates widespread restructuring of higher trophic levels in marine food webs was well underway when the K/Pg mass extinction took place.

## 1. Introduction

Marine ecosystems were dominated by reptiles during the entire Mesozoic [1–3]. Despite important turnovers at its base [4,5], the Late Cretaceous is no exception, as mosasaurid squamates rapidly diversified [6,7], achieving a cosmopolitan distribution prior to the Campanian (*ca* 83.5 Mya) [6,8], and colonized several ecological guilds until their global extinction at the Cretaceous–Palaeogene (K/Pg) boundary mass extinction (66 Mya) [7,9]. Prior to the Campanian, mosasaurid taxonomic richness saw a steep increase [6], with speciation in the Western Interior Seaway (WIS) in central North America triggering a diversification during the so-called ‘Niobraran Age’ [10,11]. High taxonomic richness persisted through the mid-Campanian [12], where an abrupt taxonomic turnover is observed in central North America at the onset of the ‘Navesinkian Age’ [11]. The abrupt shift observed in the WIS mosasaurid community is echoed in northern Europe [13], Japan [14,15], South America [16], and to some extent in Oceania [16]. Mosasaurids seem to maintain a high diversity throughout the Maastrichtian, yet with varying assemblages [17]. Despite abundant remains, it is unknown whether

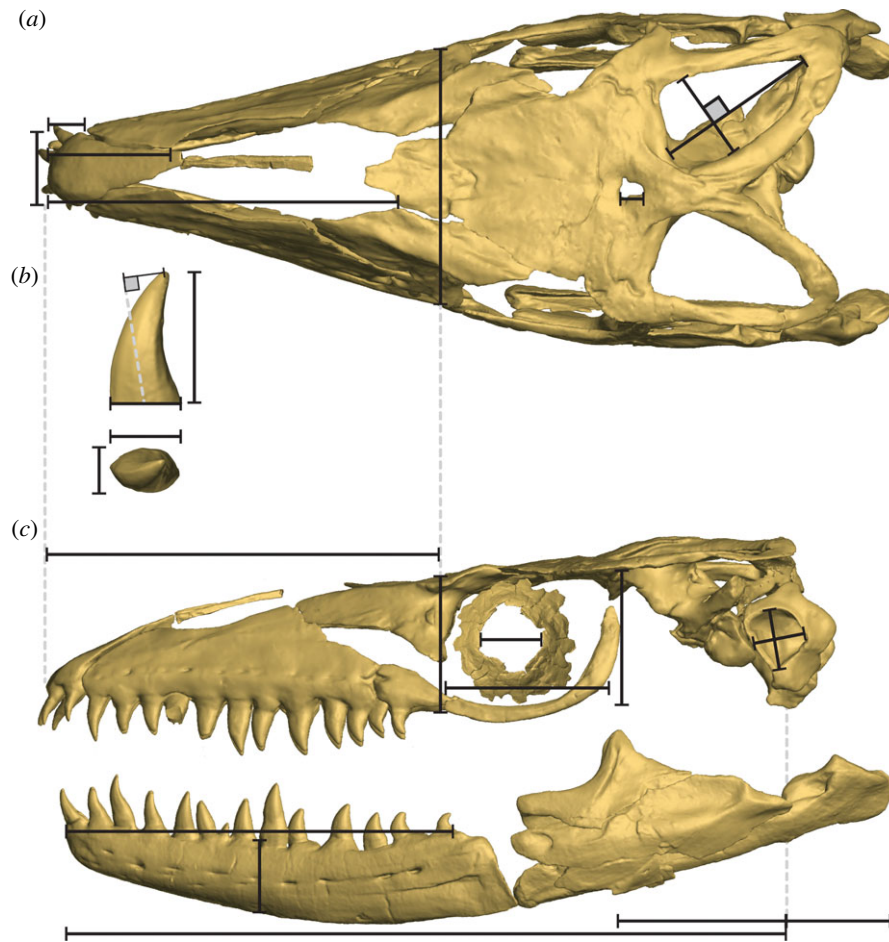


**Figure 1.** Linear measurements of the mosasaurid skull were used for quantitative trait comparisons and disparity analyses. Measurements on the skull and exemplar dentition are shown: (a) skull in dorsal aspect, (b) dentition in lateral and occlusal aspect, and (c) skull in left lateral aspect. Filled squares denote measurements taken perpendicular to one another or to the edge of a bone. Black lines describe measurements used for trait quantification; dotted grey lines are used to clarify where specific measurements are recorded from and to. Functional traits and their ecomorphological importance are presented in table 1. Linear measurements are detailed in the electronic supplementary material, figure S1. Models based on IRSNB R33b *Prognathodon solvayi*. (Online version in colour.)

these local changes in taxonomic composition resulted in constriction of functional or ecomorphological variation of these top oceanic predators on provincial or global scales leading up to the end-Cretaceous mass extinction.

Here, we explore global mosasaurid ecomorphological variation throughout the final chapter of the Mesozoic (84–66 Ma) at both local and global scales, using a set of cranial measurements including data from 37 high-precision three-dimensional models (figure 1). Because of the strong conservative forces governing mosasaurid bauplan evolution (e.g. hydrodynamic performance and phyletic heritage, e.g. [3]), we did not anticipate significant temporal changes in craniodental morphofunctional disparity, nor did we expect declines in disparity leading to the end-Cretaceous (in line with previous studies on mosasaurid craniodental disparity [3,7]). Yet, our results demonstrate polarization of ecomorphospace occupation accompanied by significant decreases in disparity, with the consequent restructuring of mosasaurid communities just before the K/Pg mass extinction, most notably in the Northern Hemisphere.

## 2. Methodology

### (a) Taxonomic and morphological sampling

Skull and jaw material from 93 mosasaurid specimens were collected, representing 56 species and all subfamilies and tribes

[6,18]. Previous studies have focussed on mosasaurid mandible form and function [3,7]; here we chose an approach quantifying function across the entire skull. Due to the current lack of a phylogeny resolving the placement of all taxa represented in this study, and because our analyses focus on global to regional patterns, we opted against the inclusion of a composite phylogenetic tree in favour of broad-scale clade assignments. The taxonomic composition of mosasaurid clades in this study follows the results of Simões *et al.* [18]; we consider halisaurines as basal mosasaurids and treat Russellosaurina (including Tethysaurinae, Tylosaurinae, Plioplatecarpinae and Yaguarasaurinae) and Mosasaurina (including Mosasaurini and Globidensini, after [19]) as monophyletic groups. Morphometric information was collected from two main sources: three-dimensional laser and structured light surface scans, as well as photogrammetric models, were the preferred methodology. Laser scanned specimens were digitized using a Creaform HandySCAN 300 handheld laser scanner at resolution 0.2–0.5 mm; structured light scanning was performed using an Artec Eva handheld scanner, at resolution 0.5 mm; photogrammed models were captured using a Nikon D3000 DSLR camera (burst mode with light-ring), with three-dimensional models generated using Agisoft Metashape 1.6.3., scaled in MeshLab 2020.06 [20]. Three-dimensional data were supplemented with two-dimensional published images and first-hand photographs (see electronic supplementary material, Information S1: specimen list for metadata). All three-dimensional models are available on MorphoSource (project ID: 000398695).

**Table 1.** Functional traits derived from linear measurements of mosasaurid skulls and jaws. Definitions, calculations and diagrammatic representations for each trait can be found in the electronic supplementary material, Information S3: functional ratios. % cov. = percentage of specimens represented by each trait. Percentages in *italics* fall outside the completeness threshold of 40%.

character	function	% cov.
jaw depressor lever arm ratio	proxy for jaw-opening mechanical advantage	77.2
jaw adductor lever arm ratio	proxy for jaw-closing mechanical advantage	73.7
functional tooththrow	defines proportion of jaw used for prey capture/processing	89.5
jaw robusticity	proxy for jaw bending resistance	85.9
supratemporal fenestra area	cross-sectional area of jaw adductor muscles	77.2
longirostry	defines hydrodynamic potential of pre-orbital snout	87.7
gullet size	proxy for volume of water expulsion, prey size etc.	80.7
tooth crown shape	proxy for tooth narrowing; hard versus soft food items	96.5
tooth blade shape	describes dental compression; conical versus blade-like teeth	61.4
tooth crown curvature	describes dental curvature	96.5
nares position	proxy for ease of inhalation during steady-state swimming	78.9
relative orbit size	defines importance of vision for taxon	75.4
pupil size (sclerotic ring diameter)	defines amount of light able to enter the pupil	15.8
tympanic resonator area	proxy for area of quadrate available as resonator	73.7
premaxillary elongation	proxy for area available for anterior pressure sensation	75.4
parietal foremen	proxy for relative size of pineal eye	70.2

### (b) Linear measurements and functional ratios

Twenty-four linear measurements were taken across the mandible, cranium and dentition (figure 1; electronic supplementary material, figure S1). Linear measurements on three-dimensional scans were taken using MeshLab 2020.06; measurements on two-dimensional images were performed in ImageJ [21]. These measurements were then used to generate 16 ratios describing the craniodental architecture and functional capacities (table 1). All these traits have clearly established functional importance or outcomes (figure 1; for further details, see electronic supplementary material, S3: functional ratios). Examples include the ratio of mandibular lever arms (proxies for mechanical advantage, i.e. ratio of muscular input force to output force on prey items), supratemporal fenestrae area (proxy for cross-sectional area of combined jaw adductor musculature) and relative orbit size (amount of the skull dedicated to visual acuity).

All 56 taxa cleared the 40% trait completeness threshold we established beforehand (a limit consistent with recent studies [4,22,23]); the dataset contains only 18.2% missing data (percentages of missing data per species can be found in electronic supplementary material, S4: species coverage). Trait ratios were standardized using a z-transformation to assign all characters a mean of 0 and a variance of 1; data were used to compute a Euclidean distance matrix for ordination analyses and disparity calculation.

### (c) Ecomorphospaces

Ordination of trait data was visualized in two dimensions in two ways: a principal coordinates analysis (PCoA) and a non-metric multi-dimensional scaling approach (NMDS). NMDS are used for visualization here as they pack more variation of the data into a two-dimensional graph, with an associated stress value for a given number of axes (see electronic supplementary material, figure S2). However, as NMDS coordinates are not ideal to use for quantitative analyses due to their non-metric properties, PCoA results were chosen for assessment of disparity. PCoAs

were performed using a cailliez correction criterion to correct for negative eigenvalues (using ape v. 5.3 [24] and were preferred to principal components analysis as PCoA allows missing values in the Euclidean distance matrix. Comparisons between PCoA and NMDS ordination demonstrated comparable patterns of ecomorphospace occupation. NMDS analyses were performed in 'vegan' v. 2.5-6 [25]; graphical results from PCoA ecomorphospaces can be found in the electronic supplementary material, figure S3. Kernel two-dimensional density estimates were used to visualize density-based macroevolutionary landscapes through time, plotted onto NMDS ecomorphospaces from Campanian to Maastrichtian, following the methodology of Fischer *et al.* [4]). Mandible length (proxy for body size) was used both in scaling datapoints to visually inspect the spread of large-sized mosasaurids and additionally to compare the spread of body sizes in mosasaurids through the Campanian–Maastrichtian.

### (d) Disparity

Morphofunctional disparity was calculated based on PCoA axes. In this study, we take an unprecedented regional and global approach to quantifying marine reptile disparity. The selection of geographic regions in this study reflects four of the most well-known and well-sampled assemblages of mosasaurids and enables the investigation and interpretation of local and global drivers of marine reptile ecomorphological variation: the WIS; Northern Tethys Province (NTP); Southern Tethys Province (STP; [26]) and Weddellian Province (consisting of Southeast Oceania, the Antarctic peninsula and Patagonia; WED). Disparity was measured through time, focusing on time bins bearing mosasaurid fossils during the latest Cretaceous: early Campanian (83.60–77.85 Mya,  $n = 34$  spp.); late Campanian (77.85–72.10 Ma,  $n = 31$  spp.); early Maastrichtian (72.10–69.05 Ma,  $n = 38$  spp.) and late Maastrichtian (69.05–65.50 Ma,  $n = 26$  spp.). The focus was made on these time periods as they encompassed the mosasaurid taxonomic turnover in the mid-Campanian and enabled the investigation of disparity in the lead up to the end-Cretaceous mass extinction. Total disparity within mosasaurid clades and



geographic regions during these time periods was also calculated. Disparity analyses were performed in R using the *disparity* package (v. 1.5.0) [27]. The sum of variances (SoV) disparity metric was preferred, as it demonstrates robusticity to sample size variation between time bins [28], but pairwise dissimilarity (PD) and sum of ranges (SoR) were also tested (table 1; electronic supplementary material, table S1). Bootstrap iterations were set at 1000 replications; additional bootstrapping procedures were performed to account for false-positive results (see electronic supplementary material, table S2). Here, we adapt the terminology from population ecology to assess disparity at the regional level (here termed ' $\alpha$ -disparity') and global level (' $\gamma$ -disparity'). In order to examine how mosasaurid ecomorphological disparity was differentiated across regional communities,  $\gamma$ -disparity per time bin was divided by mean  $\alpha$ -disparity across all provinces per time bin (see e.g. [29]), creating ' $\beta$ -disparity'. Beta-disparity can be defined as a measure of disparity differentiation; a high  $\beta$ -disparity indicates a greater range of mean  $\alpha$ -disparity values within a specific time bin, whereas low  $\beta$ -disparity indicates more uniformity in mean  $\alpha$ -disparity values, suggesting less ecomorphological differentiation between disparities across communities. Mean bootstrap iteration values were used for  $\alpha$ - and  $\gamma$ -disparity calculations and compared through four time bins (early Campanian; late Campanian; early Maastrichtian; late Maastrichtian). Changes in disparity between subsequent time bins and between clades/geographic regions were tested for using non-parametric Wilcoxon tests [30], with Bonferroni corrections for multiple comparisons.

### 3. Results

#### (a) Morphospace occupation

We quantified mosasaurid craniodental disparity from the early Campanian through the late Maastrichtian. Our aims were to establish whether faunal transitions yielded changes in disparity in mosasaurids as well as the state of global and provincial mosasaurid disparity prior to the end-Cretaceous mass extinction. Most notably, large 'megapredatory' taxa with cutting dentition, including almost all tylosaurines (figure 2a; filled purple squares) and the majority of large mosasaurines, group together in the ecomorphospace (figure 2a). These results suggest that overall skull functional morphology within these two (occasionally contemporaneous) clades of megapredatory marine reptiles converged, despite distant phylogenetic relatedness. Several brevirostrine mosasaurines occupy regions of positive NMDS axis 1, typified by relatively large supratemporal fenestrae, deep jaws, blunt rostra and crushing dentition (e.g. *Globidens* spp.). The upper half of the ecomorphospace (positive values along NMDS axis 2) is occupied predominantly by primitive mosasaurids (halisaurines and tethysaurines) and *Plioplatecarpus* spp., which all had relatively large orbits, gracile skulls and recurved, piercing teeth (figure 2a; see also electronic supplementary material, figure S3A); they constitute our 'grasping' group (figure 2a,e).

The density of ecomorphospace occupation through time (figure 2b–e) reveals a series of changes across the Campanian–Maastrichtian interval. Many mosasaurines and rulllosaurines occupy a large 'megapredatory' region through the early Campanian to the early Maastrichtian. The majority of rulllosaurines disappear afterwards, strongly altering the pattern of ecomorphospace occupation (figure 2e) by creating a clear divide between two main ecomorphologies in the late Maastrichtian bin: the 'megapredatory' group, formed predominantly by *Tylosaurus* and *Mosasaurus*, and the

'grasping' group, formed by *Plioplatecarpus*, halisaurines and several Weddellian taxa. In addition to this polarization of mosasaurid craniodental shape, a few taxa are clearly grouped in longirostrine (e.g. *Gavialimimus*) and brevirostrine (likely durophagous; e.g. *Globidens* spp.) ecomorphologies (figure 2a,b). Clade disparity appears coupled to taxonomic diversity, but nevertheless add support to the ecomorphospace signal with decreases in tylosaurine, plioplatecarpine and mosasaurin disparity through the Maastrichtian using multiple disparity metrics (electronic supplementary material, figure S4).

#### (b) Evolution of skull size

Changes in mosasaurid communities also resulted in slight variation in skull size distributions (proxy for body size) across the Campanian–Maastrichtian interval (figure 2f). early Campanian size distribution is notably more uniform, with comparable densities of large and small mosasaurids (figure 2f; blue line). By comparison, density of smaller species is lower in the late Maastrichtian, leading to a peak in mid-sized and very large species (figure 2f; yellow line). This pattern tracks the presence of multiple very large late Maastrichtian tylosaurines and mosasaurines (a pattern mirrored in sharks; [17]), and highlights the extinction of smaller species which were abundant during the Campanian (e.g. *Clidastes* and *Plesioplatecarpus*) (figure 2b,c). However, these differences are not significant, indicating that the changes in ecomorphospace occupation and disparity we observe are not associated with strong changes in mosasaurid sizes, but rather with the functional capacities of their skulls.

#### (c) Spatio-temporal evolution of disparity

We find a significant increase in global ( $\gamma$ ) ecomorphological disparity in mosasaurids (figure 3a) coincident with taxonomic turnovers known to have occurred at the mid-Campanian boundary. The observed increase in  $\gamma$ -disparity is common across all disparity metrics we computed (SoV, SoR, PD; table 2; electronic supplementary material, table S3). Our results demonstrate that  $\gamma$ -disparity of mosasaurid ecomorphologies increased from early to late Campanian and continued increasing until the early Maastrichtian, mirroring the expansion of the craniodental ecomorphospace occupation (figure 2b–d). Mosasaurid diversity (in this sample) somewhat tracks fluctuations in disparity, but not to the same magnitude (figure 3). By the late Maastrichtian,  $\gamma$ -disparity is higher than that recorded throughout the Campanian, despite fewer species being present in the late Maastrichtian (figure 3a and table 2).

While disparity increases on global ( $\gamma$ ) and provincial ( $\alpha$ ) scales from the Campanian to the Maastrichtian (table 2), we observe significant declines in  $\gamma$ -disparity from early to late Maastrichtian leading up to the K/Pg mass extinction (figure 3a–e). When examined at the provincial level (figure 3b–e), the early–late Maastrichtian transition records declines in  $\alpha$ -disparity for all provinces (with the exception of STP; table 2) using almost all disparity metrics, reinforcing the global outlook of a significant decline in ecomorphological disparity in mosasaurids in the latest Maastrichtian. This disparity decrease is found within all well-sampled clades as well, no matter the disparity metric used, except for the PD metric which slightly increased for the hyper-disparate group *Globidensini* through the Maastrichtian (figure 2d,e). Sharp decreases in tylosaurine and plioplatecarpine presence in the WIS contribute to the decline in  $\alpha$ -disparity in this region; by

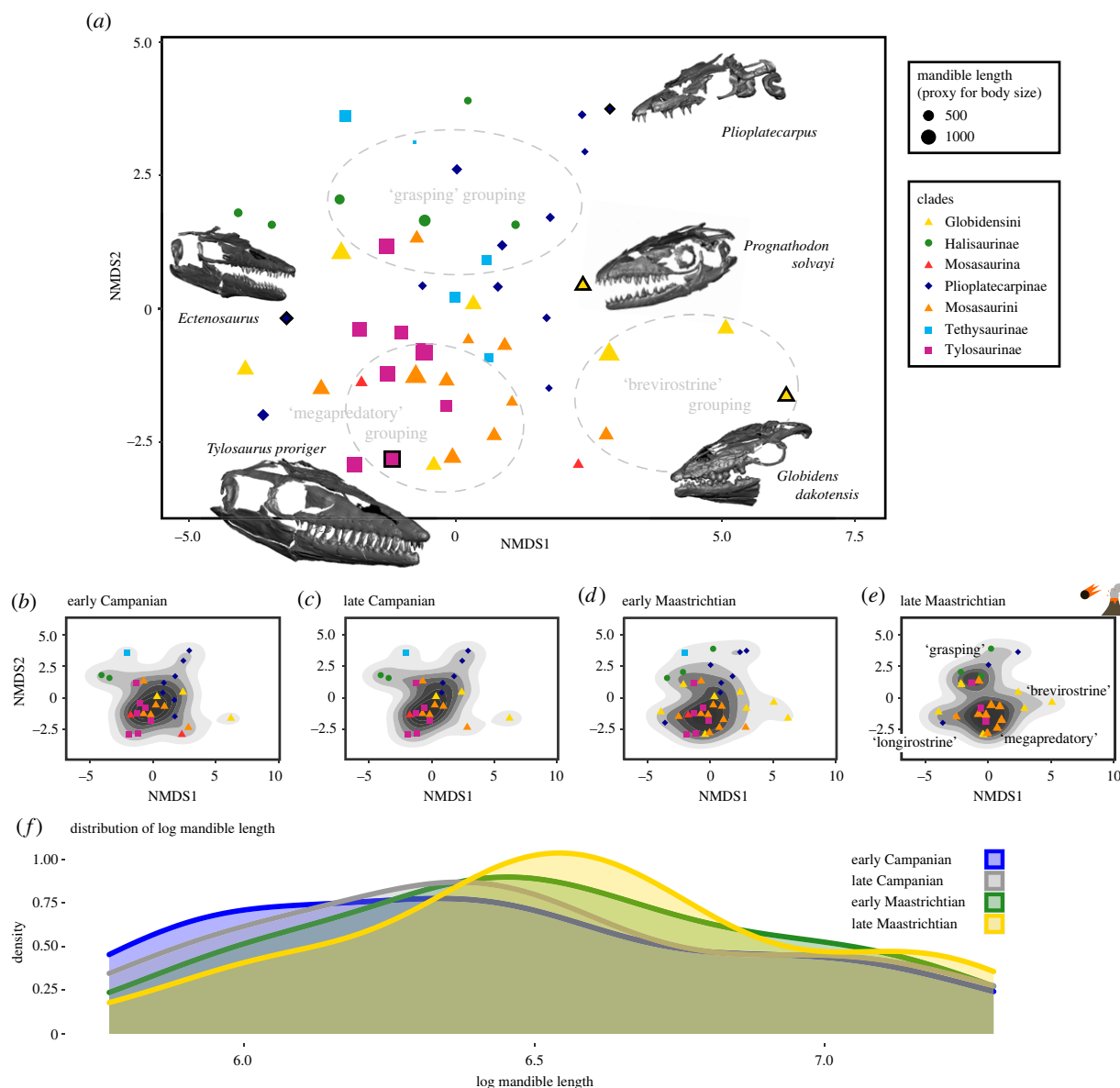


**Figure 2.** Functional ecomorphospace and size distribution in mosasauids. Functional ecomorphospace occupation (based on NMDS axes;  $k = 2$ ; stress = 0.239) by all mosasauids in the sample (a) with ecomorphological clusters and representative three-dimensional models of skulls. Data points outlined in bold represent the placement of exemplar skulls; data point size represents relative skull size (based on mandible length). Functional ecomorphospace for each time bin through the Campanian–Maastrichtian (b–e) demonstrating changes in density and isolation of ecomorphological clusters in late Maastrichtian (e). Size distribution of mosasauids through the Campanian–Maastrichtian (f) demonstrating shifts in the density of small and mid-sized mosasauids from early Campanian (ECam) to late Maastrichtian (LMaa). (Online version in colour.)

contrast, the presence of highly disparate globidensins in the STP contributes toward more stable overall  $\gamma$ -disparity during the Maastrichtian (figure 3a,d). Differentiation of disparity across regions (i.e.  $\beta$ -disparity) increases from early to late Maastrichtian (table 2) and can be attributed to several factors: decreases in  $\alpha$ -disparity in several (but crucially, not all) observed provinces; reductions in taxon count (figure 3b–e); decreased occupancy of previously commonly exploited niches (e.g. reduction of 'megapredators'; figure 2e); and increased endemism (e.g. Moroccan fauna of the STP; [19,31–33]).

## 4. Discussion

### (a) The necessity for regional and global assessments of pre-extinction diversity and disparity

The influence of localized faunal assemblages in the fossil record is well known to affect global patterns diversity and disparity

[34–37]. For many groups of large tetrapods, the global fossil record is not well resolved, whereas regional sampling in certain geographic areas is strong, and consequent global biodiversity/disparity estimates can be heavily reliant on those few regions [34,38]. In many studies, including ours, it is clear that the sampling effort in North America over the past 150 years is an important factor in estimating pre-Maastrichtian tetrapod diversity and disparity [36,39,40]. Regional diversity patterns are thus likely to contain an important signal, as the highly fragmented world of the Mesozoic and Cenozoic likely resulted in ecosystems with distinct environmental parameters [41]. This reality has often been overlooked when analysing tetrapod diversity and disparity patterns leading up to and across the K/Pg mass extinction. Indeed, a series of studies on the extinction of non-avian dinosaurs have recovered conflicting results [37,39,40,42,43], notably because of their varying treatment of regional differences and their sampling.

The fossil record of mosasauids appears only weakly biased [12], and marine reptile sampling indicators are

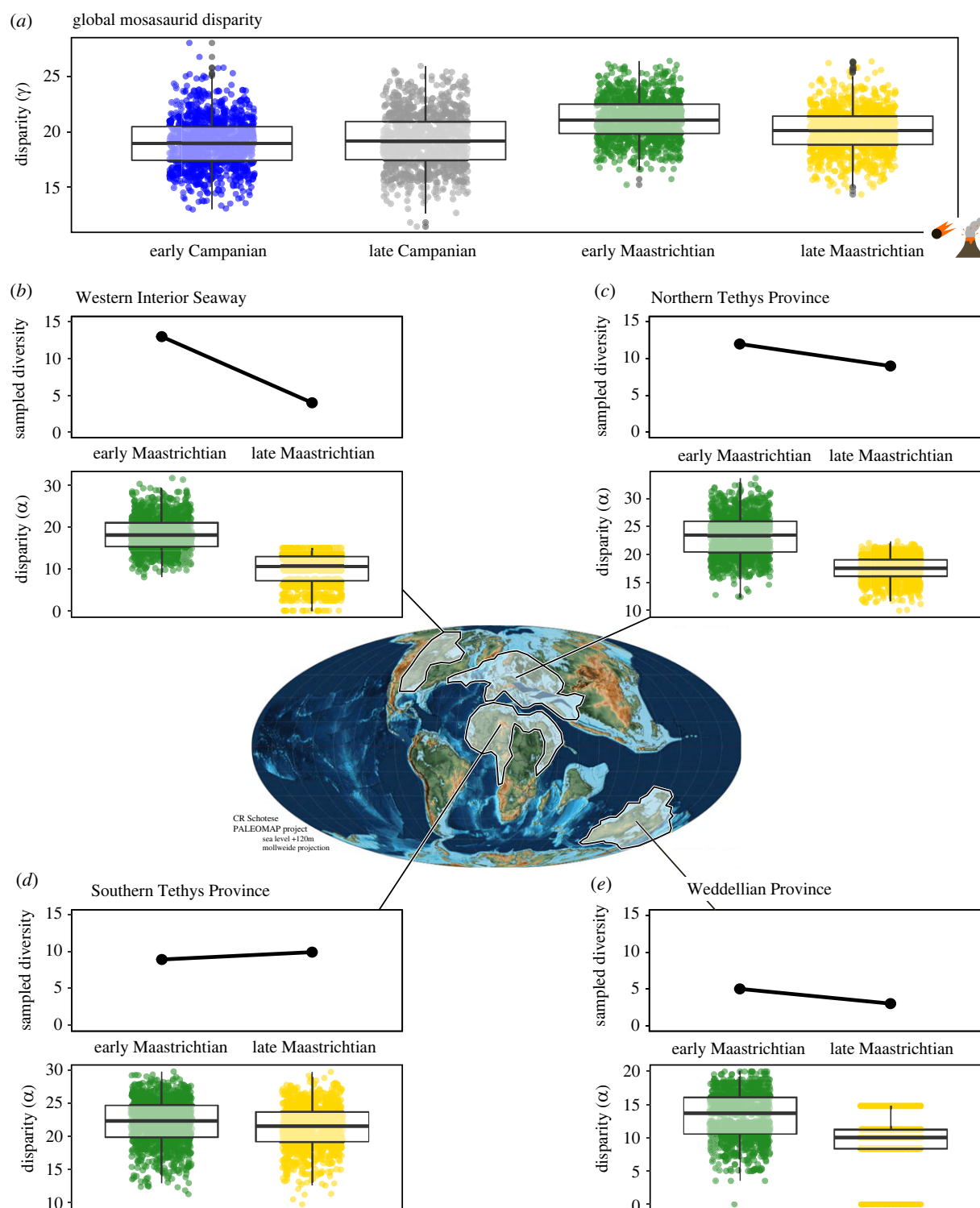


**Figure 3.** Global and provincial mosasaurid craniodental disparity through time. Global ( $\gamma$ ) craniodental disparity of mosasaurids from early Campanian to late Maastrichtian (a) presented alongside raw sample diversity and provincial ( $\alpha$ ) disparity for the Maastrichtian of the WIS (b), Northern (c) and Southern (d) Tethys Provinces, and Weddellian Province (e). Approximate extent of provincial regions projected onto a palaeomap, estimated for mid-Maastrichtian (72 Ma). Disparity estimates were generated using the SoV metric (1000 bootstrap replications); significant differences were recovered between all sequential time bins for global and provincial datasets using pairwise Wilcoxon testing (see also electronic supplementary material, tables S1 and S3). The palaeomap was provided by CR Schotese (PALEOMAP atlas for ArcGIS). (Online version in colour.)

generally excellent for the Campanian–Maastrichtian interval [5]. Our results clearly indicate regional variations in the ecomorphological disparity patterns of mosasaurids not recovered in previous ecomorphological studies of the group, potentially due to the incorporation of a coarser time-binning protocol, e.g. [3,7,44]. The drivers of ecomorphological differences we observe should not necessarily be regarded as global; a telling example is the provincial

disparity patterns during the Maastrichtian (figure 3b–e), which may be associated with the magnitude of the environmental changes resulting from the sea-level regressions [6]. Indeed, the epicontinental WIS greatly changed in extent and shape during the Maastrichtian [45,46], and this region records the steepest decrease in  $\alpha$ -disparity, while deeper basins such as Northern and STPs were seemingly less affected [8,13,26,47]. In this context, focussing on the

**Table 2.** Mosasaurid population disparity (alpha, gamma and beta) from early Campanian to late Maastrichtian. Three disparity metrics were used, with 1000 bootstrap replications. Highest mean disparity values highlighted in bold. WIS = Western Interior Seaway; NTP = Northern Tethys Province; STP = Southern Tethys Province; WED = Weddellian Province. Provincial disparities are in *italics*; highest disparity values highlighted in bold.

disparity		early Campanian	late Campanian	early Maastrichtian	late Maastrichtian
SoV					
gamma ( $\gamma$ )		18.90	19.30	<b>21.19</b>	20.12
alpha ( $\alpha$ )	mean	15.94	16.17	<b>19.26</b>	14.63
	WIS	<i>18.43</i>	<b>19.57</b>	<i>18.52</i>	9.76
	NTP	<i>22.03</i>	<i>21.60</i>	<b>23.35</b>	<i>17.50</i>
	STP	<i>10.22</i>	<i>10.44</i>	<b>22.04</b>	<i>21.51</i>
	WED	<i>13.07</i>	<i>13.06</i>	<b>13.13</b>	9.75
beta ( $\beta$ )		1.186	1.194	1.100	<b>1.375</b>
SoR					
gamma ( $\gamma$ )		68.26	64.92	<b>75.72</b>	67.49
alpha ( $\alpha$ )	mean	35.42	34.80	53.35	34.77
	WIS	<b>55.94</b>	<i>53.01</i>	<i>53.50</i>	23.64
	NTP	<i>44.42</i>	<i>44.23</i>	<b>56.49</b>	<i>45.48</i>
	STP	<i>8.78</i>	<i>9.51</i>	<i>49.93</i>	<b>51.33</b>
	WED	<b>32.53</b>	<i>32.46</i>	<i>32.25</i>	<i>18.63</i>
beta ( $\beta$ )		1.92	1.86	1.57	<b>1.94</b>
PD					
gamma ( $\gamma$ )		5.84	5.85	<b>6.27</b>	6.01
alpha ( $\alpha$ )	mean	4.63	4.75	5.71	4.72
	WIS	<i>5.65</i>	<b>5.91</b>	<i>5.76</i>	3.65
	NTP	<i>5.97</i>	<i>6.06</i>	<b>6.35</b>	<i>5.47</i>
	STP	<i>2.52</i>	<i>2.50</i>	<b>6.19</b>	<i>6.12</i>
	WED	<i>4.41</i>	<i>4.51</i>	<b>4.54</b>	3.65
beta ( $\beta$ )		1.26	1.23	1.09	<b>1.27</b>

abundant North American record to reconstruct the global diversity or disparity patterns of mosasaurids would result in a steeper late Maastrichtian decrease than that which was computed for other regions, hence confounding regional and global factors at play prior to the K/Pg mass extinction.

## (b) Pre-Cretaceous–Palaeogene mosasaurid turnovers and crises

The ‘Niobraran–Navesinkan’ (early to late Campanian) taxonomic transition from ruseselosaurine-to-mosasaurine-dominated communities was initially identified in the WIS [11,48] and notably involved selective extinction of smaller taxa. Since then, similar turnovers have been identified in multiple other regions across the globe [13–16], yet without clear reductions of smaller species [13,49]. We show that, far from experiencing a global  $\gamma$ -disparity decline during this turnover, mosasaurids increased in disparity across this transition (non-significantly using SoR metric, significantly using the SoR and PD metrics; electronic supplementary material, table S3). This increase is likely in part due to the extinction of more ‘generalist’ and small-sized pliolatecarpines and tylosaurines (figure 3a). These extinctions in the WIS reduced the density of ‘megapredatory’ and ‘generalist’

ecomorphologies in the late Campanian bin (figure 2b,c), causing increased polarization of the remaining phenotypes exhibited by mosasaurid taxa. Actually, the increase in morphofunctional disparity at the ‘Niobraran–Navesinkan’ transition is a phenomenon local to the WIS, with a high enough amplitude to influence global patterns; other regions maintain stable morphofunctional disparity through this interval (figure 3 and table 2) while experiencing similar taxonomic composition shifts, e.g. [13,15,16]. Within the North American continent, evidence from western and central Alabama not only support the abrupt shift in taxon abundance at the Niobraran–Navesinkan transition, but also highlight the likelihood of community segregation and habitat partitioning prior to this transition within the ruseselosaurine-dominated communities [11]. The cause behind the abrupt shift in mosasaurid community composition across the ‘Niobraran–Navesinkan’ is as yet unclear. A decrease in global oceanic temperature between the mid- and late Campanian is coincident with the turnover [6,50]. Such a shift in temperatures would have affected multiple habitats, potentially driving a pre-Maastrichtian restructuring of marine reptile communities in deep- and shallow-water biomes [11]. High global sea levels in the mid-Campanian may have played a role in maintaining ecomorphological stability on a global scale [6], although recent analyses



suggest physical drivers did account for large-scale patterns of mosasaurid morphofunctional disparity [7]. The onset of localized regressions (e.g. triggered by the Laramide Orogeny in the WIS [46]) may have promoted ecomorphological diversification in the wake of population/community isolation there [11]. Such an effect would be consistent with our mid-Campanian disparity results for the WIS (table 2), although assigning it as a causative agent is highly speculative at present, especially for taxa likely possessing high dispersal capabilities such as derived mosasaurids [51].

We do not find evidence for a long-term ecomorphological decline of mosasaurids across the entire Campanian–Maastrichtian interval, as the early Maastrichtian is identified here as the time of greatest  $\gamma$ -disparity of mosasaurids (figure 3a). This time interval witnessed the expansion of ecomorphospace occupation by longirostrine and brevirostrine mosasaurid ecomorphologies, in addition to the diversification of ‘grasping’ halisaurines and plioplatecarpines (figure 2A + D). In studies using coarser temporal and geographic frameworks [7], this would result in high mosasaurid disparity up to the K/Pg extinction. Our time-binning approach recovers a within-Maastrichtian decrease in global  $\gamma$ -disparity and  $\alpha$ -disparity, in nearly all regions and across all clades. When the differentiation of ecomorphological disparity between geographical regions is considered (i.e.  $\beta$ -disparity; table 2), it is clear that the late Maastrichtian was a time of increased regionalization of mosasaurid disparity, rather than a consistent, globalized decline. Communities of mosasaurids in the WIS, NTP and WP are shown to be notably more phenotypically homogeneous in the late Maastrichtian than those of the early Maastrichtian (figure 3b–e), with the WIS and WED communities represented by few taxa within only two tribes (Mosasaurini + Globidensini, and Mosasaurini + Tylosaurini, respectively). By contrast, the late Maastrichtian mosasaurid community of the STP comprised an ecomorphologically diverse assemblage of globidensins (e.g. *Globidens* and *Prognathodon*), mosasaurins (*Mosasaurus* and *Eremiasaurus*), halisaurines (e.g. *Pluridens* and *Halisaurus*) and plioplatecarpines (e.g. *Gavialimimus*) [19,31,33], yielding a high  $\alpha$ -disparity in this region (figure 3d). The retention of disparate ecomorphologies of STP mosasaurids through the Maastrichtian drive peak in provincial differentiation (table 2). The predominantly bimodal landscape of mosasaurids in the late Maastrichtian (figure 2e) suggests that, while a variety of niches were still being occupied by low densities of disparate mosasaurids, numerous Northern and Southern Tethys mosasaurids essentially exhibited ‘megapredatory’ or ‘grasping’ functional adaptations (figure 2; also [7,8,13,26]). Becoming increasingly apparent is the importance of the STP (including Afro-Arabia, Morocco, Niger–Nigeria, Angola and eastern Brazil) in driving the late Maastrichtian marine reptile diversity and disparity [26]. Understanding patterns such as these are vital for the accurate interpretation of faunal dynamics and functional variation before and after extinction events. If only  $\gamma$ -disparity of mosasaurids were considered, then this group could be simply interpreted as experiencing a global ecomorphological decline just prior to their ultimate demise at the K/Pg boundary (or not in decline at all if a single and global ‘Maastrichtian’ bin was used; see [7]). However, it is apparent that, when both  $\alpha$ - and  $\beta$ -disparities are taken into account, some regional communities were most certainly declining in taxonomic diversity and ecomorphological

disparity, whereas others were only minimally affected on both counts.

### (c) How selective are the pre-Cretaceous–Palaeogene extinctions in marine reptiles?

Ichthyosaurs and pliosaurs were long gone by the Maastrichtian [4,5,52], restricting the predominant marine reptile groups to xenopsarian plesiosaurs, mosasaurids, chelonoids and crocodylomorphs [8]. These clades do not seem to follow a disparity pattern similar to that recovered here or elsewhere [7] for mosasaurids. Indeed, polycotyloid plesiosaurs were already in decline in both phylogenetic diversity and ecomorphological disparity during the Campanian–Maastrichtian interval [22], with only two species potentially being present during the Maastrichtian [22,53]. Robust evaluations of elasmosaurid disparity are still lacking, but the range of phenotypes (either in terms of phylogenetic diversity, osteology or relative neck length) appears to still be broad during the Maastrichtian [54], although within-Maastrichtian changes have not yet been computed. Similarly, within-Maastrichtian disparity dynamics have not been explored for marine testudines, although previous assessments of testudines indicate a peak in cranial morphological variation in the Maastrichtian [55], and a consistent contribution to the diversity of feeding morphologies across marine reptiles from Campanian to Maastrichtian [3]. By contrast, aquatic crocodylomorphs exhibit comparatively low and declining disparity during the latest Cretaceous [56], with the exception of dyrosaurid tethysuchians, which exhibited a rapid burst of morphological evolution during the Maastrichtian [56]. The increased endemism and expansion into ‘grasping’ and ‘longirostrine’ ecomorphologies by Southern Tethys mosasaurids in the late Maastrichtian combines with isotopic analyses of trophic structure in the Maastrichtian of the same region [9], suggesting increased dietary specialization in this region as multiple predators coexisted and often fed upon prey from a single trophic level. Patterns of taxonomic diversity and ecomorphological disparity across multiple marine reptile groups and multiple geographic regions indicate that wholesale (and in some cases fragile) restructuring of marine trophic webs was underway before the K/Pg mass extinction event, which subsequently annihilated numerous highly disparate marine reptile groups.

**Data accessibility.** Data recorded in this study are provided in the electronic supplementary material [57], Information, with measurements and converted data provided in electronic supplementary material, Excel spreadsheets. R-code used in this study is provided in the electronic supplementary material, Information; the electronic supplementary material is also provided on the Dryad Digital Repository: <https://doi.org/10.5061/dryad.x3fbbg7mc> [58]. Three-dimensional models scanned and measured during this study are available publicly on the online data repository Morphosource.

**Authors’ contributions.** J.A.M.: conceptualization, data curation, formal analysis, funding acquisition, investigation, methodology, project administration, resources, software, validation, visualization, writing—original draft and writing—review and editing; R.F.B.: data curation, formal analysis, funding acquisition, investigation, resources and writing—review and editing; N.B.: validation, and writing—review and editing; V.F.: conceptualization, data curation, formal analysis, funding acquisition, methodology, project administration, resources, software, supervision, visualization and writing—review and editing.

All authors gave final approval for publication and agreed to be held accountable for the work performed therein.



**Conflict of interest declaration.** We declare we have no competing interests.

**Funding.** This work was funded by grants from the Fonds De La Recherche Scientifique (F.R.S.-FNRS): MIS F.4511.19 'SEASCAPE' (V.F.), FNRS travel grant 35706165 (J.A.M.) and a FRIA doctoral fellowship grant FC 23645 (R.F.B.).

**Acknowledgements.** The authors would like to thank the museum curators for access to their specimens from: KUVF, Kansas; FHSN, Kansas;

USNM, Washington DC; FMNH, Chicago; UW, Laramie; FFHM, Oakley; MNHN, Paris; PMU, Uppsala; GPIT, Tübingen. We thank Annelise Folie of the Royal Belgian Institute of Natural Sciences (RBINS) for facilitating access to their imaging facility and digital data, Mike Polcyn and Narimane Chatar for additional scans. A preprint of this article was published online on bioRxiv on 1 January 2022 [59] (<https://doi.org/10.1101/2021.12.30.474572>), with a Dryad supplement available at <https://doi.org/10.5061/dryad.x3ffbg7mc>.

## References

- Reeves JC, Moon BC, Benton MJ, Stubbs TL. 2021 Evolution of ecospace occupancy by Mesozoic marine tetrapods. *Palaeontology* **64**, 31–49. (doi:10.1111/PALA.12508)
- Kelley NP, Pyenson ND. 2015 Evolutionary innovation and ecology in marine tetrapods from the Triassic to the Anthropocene. *Science* **348**, aaa3716. (doi:10.1126/SCIENCE.AAA3716)
- Stubbs TL, Benton MJ. 2016 Ecomorphological diversifications of Mesozoic marine reptiles: the roles of ecological opportunity and extinction. *Paleobiology* **42**, 547–573. (doi:10.1017/PAB.2016.15)
- Fischer V, MacLaren JA, Soul LC, Bennion RF, Druckenmiller PS, Benson RBJ. 2020 The macroevolutionary landscape of short-necked plesiosaurs. *Sci. Rep.* **10**, 16434. (doi:10.1038/s41598-020-73413-5)
- Fischer V, Bardet N, Benson RBJ, Arkhangelsky MS, Friedman M. 2016 Extinction of fish-shaped marine reptiles associated with reduced evolutionary rates and global environmental volatility. *Nat. Commun.* **7**, 1–11. (doi:10.1038/ncomms10825)
- Polcyn MJ, Jacobs LL, Araújo R, Schulp AS, Mateus O. 2014 Physical drivers of mosasaur evolution. *Palaeogeogr. Palaeoclimatol. Palaeoecol.* **400**, 17–27. (doi:10.1016/j.palaeo.2013.05.018)
- Cross SRR, Moon BC, Stubbs TL, Rayfield EJ, Benton MJ. 2022 Climate, competition, and the rise of mosasauroid ecomorphological disparity. *Palaeontology* **65**, e12590. (doi:10.1111/PALA.12590)
- Bardet N, Houssaye A, Vincent P, Pereda Suberbiola X, Amaghaz M, Jourani E, Meslouh S. 2014 Mosasaurids (Squamata) from the Maastrichtian phosphates of Morocco: biodiversity, palaeobiogeography and palaeoecology based on tooth morphoguilds. *Gondwana Res.* **27**, 1068–1078. (doi:10.1016/j.gr.2014.08.014)
- Martin JE, Vincent P, Tacail T, Khaldoune F, Jourani E, Bardet N, Balter V. 2017 Calcium isotopic evidence for vulnerable marine ecosystem structure prior to the K/Pg extinction. *Curr. Biol.* **27**, 1641–1644.e2. (doi:10.1016/j.cub.2017.04.043/ATTACHMENT/09B06FB7-54D0-4121-A985-7D93C049CDB1/MMC1.PDF)
- Russell DA. 1967 Systematics and morphology of American mosasaurs. In *Bulletin of the Peabody Museum of Natural History, Yale University, USA*, pp. 1–242. Connecticut, NJ: Yale University.
- Kiernan CR. 2002 Stratigraphic distribution and habitat segregation of mosasaurs in the Upper Cretaceous of western and central Alabama, with an historical review of Alabama mosasaur discoveries. *J. Vertebr. Paleontol.* **22**, 91–103. (doi:10.1671/0272-4634(2002)022[0091:SDAHSO]2.0.CO;2)
- Driscoll DA, Dunhill AM, Stubbs TL, Benton MJ. 2019 The mosasaur fossil record through the lens of fossil completeness. *Palaeontology* **62**, 51–75. (doi:10.1111/pala.12381)
- Lindgren J. 2004 Stratigraphical distribution of Campanian and Maastrichtian mosasaurs in Sweden: evidence of an intercontinental marine extinction event? *GFF* **126**, 221–229. (doi:10.1080/11035890401262221)
- Tanimoto M. 2005 Mosasaur remains from the Upper Cretaceous Izumi Group of southwest Japan. *Netherlands J. Geosci. Geologie en Mijnbouw* **84**, 373–378. (doi:10.1017/S0016774600021156)
- Sato T, Konishi T, Hirayama R, Caldwell MW. 2012 A review of the Upper Cretaceous marine reptiles from Japan. *Cretaceous Res.* **37**, 319–340. (doi:10.1016/j.cretres.2012.03.009)
- Jiménez-Huidobro P, Simões TR, Caldwell MW. 2017 Mosasauroids from Gondwanan continents. *J. Herpetol.* **51**, 355–364. (doi:10.1670/16-017)
- Cappetta H, Bardet N, Pereda Suberbiola X, Adnet S, Akkrm D, Amalik M, Benabdallah A. 2014 Marine vertebrate faunas from the Maastrichtian phosphates of Benguerir (Gannour Basin, Morocco): biostratigraphy, palaeobiogeography and palaeoecology. *Palaeogeogr. Palaeoclimatol. Palaeoecol.* **409**, 217–238. (doi:10.1016/j.palaeo.2014.04.020)
- Simões TR, Vernygora O, Paparella I, Jimenez-Huidobro P, Caldwell MW. 2017 Mosasauroid phylogeny under multiple phylogenetic methods provides new insights on the evolution of aquatic adaptations in the group. *PLoS ONE* **12**, 1–20. (doi:10.1371/journal.pone.0176773)
- Leblanc ARH, Caldwell MW, Bardet N. 2012 A new mosasauroine from the Maastrichtian (Upper Cretaceous) phosphates of Morocco and its implications for mosasauroine systematics. *J. Vertebr. Paleontol.* **32**, 82–104. (doi:10.1080/02724634.2012.624145)
- Cignoni P, Callieri M, Corsini M, Dellapiane M, Ganovelli F, Ranzuglia G. 2008 MeshLab: an open-source mesh processing tool. In *Eurographics Italian chapter conference* (eds V Scarano, R de Chiara, U Erra), pp. 1–8. Salerno, Italy: The Eurographics Association.
- Schneider CA, Rasband WS, Eliceiri KW. 2012 NIH Image to ImageJ: 25 years of image analysis. *Nat. Methods* **9**, 671–675. (doi:10.1038/nmeth.2089)
- Fischer V, Benson RBJ, Druckenmiller PS, Ketchum HF, Bardet N. 2018 The evolutionary history of polycotylid plesiosaurs. *R. Soc. Open Sci.* **5**, 172177. (doi:10.1098/RSO5.172177)
- Button DJ, Zanno LE. 2020 Repeated evolution of divergent modes of herbivory in non-avian dinosaurs. *Curr. Biol.* **30**, 158–168.e4. (doi:10.1016/J.CUB.2019.10.050)
- Paradis E, Claude J, Strimmer K. 2004 APE: analyses of phylogenetics and evolution in R language. *Bioinformatics* **20**, 289–290. (doi:10.1093/bioinformatics/btg412)
- Oksanen J et al. 2018 vegan: Community Ecology Package. R package version 2.5-6.
- Bardet N. 2012 Maastrichtian marine reptiles of the Mediterranean Tethys: a palaeobiogeographical approach. *Bull. Soc. Geol. Fr.* **183**, 573–596. (doi:10.2113/gssgfbull.183.6.573)
- Guillerm T. 2018 dispRity: a modular R package for measuring disparity. *Methods Ecol. Evol.* **9**, 1755–1763. (doi:10.1111/2041-210X.13022)
- Ciampaglio CN, Kemp M, McShea DW. 2009 Detecting changes in morphospace occupation patterns in the fossil record: characterization and analysis of measures of disparity. *Paleobiology* **27**, 695–715. (doi:10.1666/0094-8373(2001)027<0695:DCIMOP>2.0.CO;2)
- Legendre P. 2008 Studying beta diversity: ecological variation partitioning by multiple regression and canonical analysis. *J. Plant Ecol.* **1**, 3–8. (doi:10.1093/JPE/RTM001)
- R Core Development Team 2008 *R: a language and environment for statistical computing*. Vienna, Austria: R Foundation for Statistical Computing. See <http://www.R-project.org/>.
- Strong CRC, Caldwell MW, Konishi T, Palci A. 2020 A new species of longirostrine pliolatocarpine mosasaur (Squamata: Mosasauridae) from the Late Cretaceous of Morocco, with a re-evaluation of the problematic taxon '*Platycarpus*' *ptychodon*. *J. Syst. Paleontol.* **18**, 1769–1804. (doi:10.1080/14772019.2020.1818322)
- Lingham-Soliar T. 2002 First occurrence of premaxillary caniniform teeth in the varanoidea: presence in the extinct mosasaur *Goronyosaurus*

- (Squamata: Mosasauridae) and its functional and paleoecological implications. *Lethaia* **35**, 187–190. (doi:10.1080/002411602320184033)
33. Longrich NR, Bardet N, Khaldoune F, Yazami OK, Jalil NE. 2021 *Pluridens serpentis*, a new mosasaurid (Mosasauridae: Halisaurinae) from the Maastrichtian of Morocco and implications for mosasaur diversity. *Cretaceous Res.* **126**, 104882. (doi:10.1016/j.cretres.2021.104882)
  34. Close RA *et al.* 2019 Diversity dynamics of Phanerozoic terrestrial tetrapods at the local-community scale. *Nat. Ecol. Evol.* **3**, 590–597. (doi:10.1038/s41559-019-0811-8)
  35. Upchurch P, Mannion PD, Benson RBJ, Butler RJ, Carrano MT. 2011 Geological and anthropogenic controls on the sampling of the terrestrial fossil record: a case study from the Dinosauria. *Geol. Soc. Lond. Special Publications* **358**, 209–240. (doi:10.1144/SP358.14)
  36. Longrich NR, Scriberas J, Wills MA. 2016 Severe extinction and rapid recovery of mammals across the Cretaceous–Palaeogene boundary, and the effects of rarity on patterns of extinction and recovery. *J. Evol. Biol.* **29**, 1495–1512. (doi:10.1111/JEB.12882)
  37. Condamine FL, Guinot G, Benton MJ, Currie PJ. 2021 Dinosaur biodiversity declined well before the asteroid impact, influenced by ecological and environmental pressures. *Nat. Commun.* **12**, 1–16. (doi:10.1038/s41467-021-23754-0)
  38. Tulin SL, Butler RJ. 2017 The completeness of the fossil record of plesiosaurs, marine reptiles from the Mesozoic. *Acta Palaeontol. Pol.* **62**, 563. (doi:10.4202/APP.00355.2017)
  39. Maidment SCR, Dean CD, Mansergh RI, Butler RJ. 2021 Deep-time biodiversity patterns and the dinosaurian fossil record of the Late Cretaceous Western Interior, North America. *Proc. R. Soc. B* **288**, 20210692. (doi:10.1098/RSPB.2021.0692)
  40. Vavrek MJ, Larsson HC. 2010 Low beta diversity of Maastrichtian dinosaurs of North America. *Proc. Natl Acad. Sci. USA* **107**, 8265–8268. (doi:10.1073/PNAS.0913645107)
  41. Zaffos A, Finnegan S, Peters SE. 2017 Plate tectonic regulation of global marine animal diversity. *Proc. Natl Acad. Sci. USA* **114**, 5653–5658. (doi:10.1073/PNAS.1702297114)
  42. Dean CD, Chiarenza AA, Maidment SCR. 2020 Formation binning: a new method for increased temporal resolution in regional studies, applied to the Late Cretaceous dinosaur fossil record of North America. *Palaeontology* **63**, 881–901. (doi:10.1111/PALA.12492)
  43. Chiarenza AA, Mannion PD, Lunt DJ, Farnsworth A, Jones LA, Kelland SJ, Allison PA. 2019 Ecological niche modelling does not support climatically-driven dinosaur diversity decline before the Cretaceous/Paleogene mass extinction. *Nat. Commun.* **10**, 1–14. (doi:10.1038/s41467-019-08997-2)
  44. Madzia D, Cau A. 2020 Estimating the evolutionary rates in mosasauroids and plesiosaurs: discussion of niche occupation in Late Cretaceous seas. *PeerJ* **8**, e8941. (doi:10.7717/peerj.8941)
  45. Berry K. 2017 New paleontological constraints on the paleogeography of the Western Interior Seaway near the end of the Cretaceous (late Campanian–Maastrichtian) with a special emphasis on the paleogeography of southern Colorado, U.S.A. *Rocky Mountain Geol.* **52**, 1–16. (doi:10.24872/RMGJOURNAL.52.1.1)
  46. Slattery J, Cobban WA, McKinnery KC, Harries PJ, Sandness AL. 2013 *Early Cretaceous to Paleocene paleogeography of the Western Interior Seaway: the interaction of eustasy and tectonism*. In *Wyoming Geological Association Handbook* (ed. M Bingle-Davis), Wyoming Geological Association 68th Annual Field Conf, Casper, Wyoming, pp. 22–60.
  47. Hornung JJ, Reich M, Frerichs U. 2018 A mosasaur fauna (Squamata: Mosasauridae) from the Campanian (Upper Cretaceous) of Hannover, northern Germany. *Alcheringa* **42**, 543–559. (doi:10.1080/03115518.2018.1434899)
  48. Nicholls EL, Russell AP. 1990 Paleobiogeography of the Cretaceous Western Interior Seaway of North America: the vertebrate evidence. *Palaeogeogr. Palaeoclimatol. Palaeoecol.* **79**, 149–169. (doi:10.1016/0031-0182(90)90110-5)
  49. Jagt JWM. 2005 Stratigraphic ranges of mosasaurs in Belgium and the Netherlands (Late Cretaceous) and cephalopod-based correlations with North America. *Netherlands J. Geosci. Geologie en Mijnbouw* **84**, 283–301. (doi:10.1017/S0016774600021065)
  50. Linnert C, Engelke J, Wilmsen M, Mutterlose J. 2016 The impact of the Maastrichtian cooling on the marine nutrient regime—evidence from midlatitudinal calcareous nannofossils. *Paleoceanography* **31**, 694–714. (doi:10.1002/2015PA002916)
  51. Lindgren J, Caldwell MW, Konishi T, Chiappe LM. 2010 Convergent evolution in aquatic tetrapods: insights from an exceptional fossil mosasaur. *PLoS ONE* **5**, 1–10. (doi:10.1371/journal.pone.0011998)
  52. Schumacher BA. 2011 A 'Woollgari Zone Mosasaur' (Squamata; Mosasauridae) from the Carlile Shale (Lower Middle Turonian) of Central Kansas and the Stratigraphic Overlap of Early Mosasaurs and Pliosaurid Plesiosaurs. *Trans. Kansas Acad. Sci.* **114**, 1–14. (doi:10.1660/062.114.0101)
  53. O'gorman JP, Gasparini Z. 2013 Revision of *Sulcusuchus erraini* (Sauropterygia, Polycotylidae) from the Upper Cretaceous of Patagonia, Argentina. *Alcheringa* **37**, 163–176. (doi:10.1080/03115518.2013.736788)
  54. Fischer V, Zverkov NG, Arkhangelsky MS, Stenshin IM, Blagovetshensky IV, Uspensky GN. 2021 A new elasmosaurid plesiosaurian from the Early Cretaceous of Russia marks an early attempt at neck elongation. *Zool. J. Linn. Soc.* **192**, 1167–1194. (doi:10.1093/ZOOLINNEAN/ZLAA103)
  55. Foth C, Ascarrunz E, Joyce WG. 2017 Still slow, but even steadier: an update on the evolution of turtle cranial disparity interpolating shapes along branches. *R. Soc. Open Sci.* **4**, 170899. (doi:10.1098/RSPB.170899)
  56. Stubbs TL, Pierce SE, Elsler A, Anderson PSL, Rayfield EJ, Benton MJ. 2021 Ecological opportunity and the rise and fall of crocodylomorph evolutionary innovation. *Proc. R. Soc. B* **288**, 20210069. (doi:10.1098/RSPB.2021.0069)
  57. MacLaren JA, Bennion RF, Bardet N, Fischer V. 2022 Global ecomorphological restructuring of dominant marine reptiles prior to the K/Pg mass extinction. FigShare. (doi:10.6084/m9.figshare.c.5986026)
  58. MacLaren JA, Bennion RF, Bardet N, Fischer V. 2022 Data from: Global ecomorphological restructuring of dominant marine reptiles prior to the Cretaceous–Palaeogene mass extinction. Dryad Digital Repository. (doi:10.5061/dryad.x3ffbg7mc)
  59. MacLaren JA, Bennion RF, Bardet N, Fischer V. 2022 Global ecomorphological restructuring of dominant marine reptiles prior to the K/Pg mass extinction. *bioRxiv*. 2021.12.30.474572. (doi:10.1101/2021.12.30.474572)